Journal of Sound and Vibration (1999) **228**(3), 683–699
Article No. jsvi.1999.2421, available online at http://www.idealibrary.com on IDEAL®

FREE VIBRATIONS OF ELLIPTICAL RINGS WITH CIRCUMFERENTIALLY VARIABLE THICKNESS

R. S. HWANG, C. H. J. FOX AND S. MCWILLIAM

School of Mechanical, Materials, Manufacturing Engineering and Management, University of Nottingham, University Park, Nottingham NG7 2RD, U.K.

(*Received* 15 *March* 1999, *and in final form* 11 *June* 1999)

This paper deals with the in-plane free vibration of rings with a nominally elliptical centreline. Results are presented for rings of constant axial length that have a rectangular cross-section, the radial thickness of which is constant or has a simple, analytically defined circumferential variation. Additionally, and for the first time, the effects of small variations in in-plane profile, such as those arising in practical rings due to manufacturing tolerances, are considered. The problem is tackled using an approach in which the true middle surface is determined numerically from the outer and inner surface profiles, which can be defined either by exact analytical expressions or in a more general way using Fourier series. The Rayleigh–Ritz method is used to obtain the natural frequencies and mode shapes. Results are presented for a range of cases, including some that have previously been studied by other authors and some that have not. The effects on frequency splitting due to profile variations and the aspect ratio of the ellipse are emphasized. Results obtained using the developed numerical approach show excellent agreement with finite element predictions.

1. INTRODUCTION

The in-plane vibration of elliptical and oval rings is a problem of some practical importance that has attracted the attention of a number of researchers in recent years although, in comparison to circular rings, the number of papers published is quite small. The present paper has three main aims. Firstly, it illustrates the application to elliptical rings of a new and quite general approach to the in-plane vibration of closed rings, the theoretical formulation of which is presented in references [1, 2] with applications to nominally circular rings reported in references [3, 4]. Secondly, it presents results relating to the effects of small circumferential profile variations superimposed on the nominal cross-sectional shape, such as those which will inevitably exist in a real elliptical ring due to manufacturing processes. This aspect has not been considered in any previous publication known to the authors. Thirdly, it extends the results for variable thickness rings, presented in reference [5], to include antisymmetric modes.

Before presenting the main content of the paper, it is useful to give a brief review of the relevant earlier publications on the topic. Brigham [6] considered the

0022-460X/99/480683 + 17 $30.00/0

vibration of oval rings. He developed force and moment equilibrium equations for oval rings of variable cross-section and reduced these to an algebraic form using a truncated trigonometric series to express the displacements. Numerical results were presented for the first few in-plane modes of a ring of uniform thickness. Sato [7] illustrated a method for the free in-plane vibration of an elliptical ring with uniform cross-section using Love's theory of thin curved rods, assuming the central line of the ring to be "inextensional". The equations of motion were expressed in elliptical co-ordinates and the displacements were represented by a series of Mathieu functions [8]. Numerical predictions of the frequencies of the first eight modes showed good agreement with experimental measurements. Laura *et al.* [5] used the Rayleigh–Ritz method to investigate the free flexural vibrations of elliptical rings that have simple variations in cross-section but retain two planes of symmetry. The geometry of the undeformed ring was described using exact analytical expressions. The natural frequency factors were calculated using three-term sinusoidal and optimized three-term polynomial functions to describe the displacement of the middle surface. Numerical results were presented for a range of values of ellipticity and thickness variations for modes which are symmetrical with respect to the planes of symmetry of the ellipse. Antisymmetric modes were not considered. The literature also contains a number of papers on the related topic of the vibration of elliptical shells of which references [9, 10] are good examples.

Note that, in references [6–10] cited above, it was assumed that the middle surface of the ring was known *a priori* in a specific analytic form. For rings of complex shape, the true middle surface will not normally be known and must be determined from the inner and outer surfaces.

In sections 2 and 3, the geometrical description of the ring is considered and a brief outline of the derivation of the frequency equation is given. Numerical results are presented in section 4 for a number of cases and, where possible, comparisons are made with previously published results. Additionally, finite element results are presented for several cases in order to provide confirmation of the results calculated using the current numerical approach.

2. GEOMETRY

The natural frequencies and mode shapes of the ring are to be calculated using the Rayleigh–Ritz method. A suitable description of the geometry of the undeformed ring is required so that the strain energy and kinetic energy can be evaluated. In references [1, 2], the inner and outer profiles of non-circular rings were described in a general way using Fourier series. When considering a perfectly elliptical ring, or indeed any ring whose inner and outer profiles can be defined by known analytical functions, there are two ways to proceed.

One may choose to describe the ring geometry in terms of the known analytical functions or one may choose to express the profiles as Fourier series. The former approach will usually be more computationally efficient, but the latter approach allows the frequency splits to be interpreted in the context of the frequency-splitting rules discussed in reference [4], which are expressed in terms of the spatial-harmonic content of the profile. Furthermore, when considering a ring that departs from the perfectly elliptical (in which case an analytical description of the profile may not be available), it is very convenient to adopt a Fourier series description for the profile. Results will therefore be presented that have been derived using both approaches.

A start is made by considering the geometry of the undeformed ring. There are two cases to consider, one where the ring is perfectly elliptical and the other where the ring deviates from perfect ellipticity by a small but significant amount.

The equation of a perfect ellipse can be expressed in rectangular co-ordinates (see Figure 1(a)) as

$$\frac{x^2}{a^2}+\frac{y^2}{b^2}=1, \tag{1}$$

where a and b are the semi-major and semi-minor axes, respectively.

It follows from Figure 1(a) that the co-ordinates of a point on the ellipse can be expressed in terms of the length OP, denoted r_P, and the angle β formed by the lines OP and OX, as

$$x = r_p \cos\beta, \tag{2}$$

$$y = r_p \sin\beta. \tag{3}$$

It follows that r_P can be expressed as

$$r_P = \frac{ab}{[a^2 \sin^2\beta + b^2\cos^2\beta]^{1/2}}. \tag{4}$$

In the case where the inner and outer profiles of the ring are perfectly elliptical, their shape can be defined by equation (4) with appropriate values of a and b, say a_i, b_i and a_o, b_o, for the inner and outer profiles, respectively. The Fourier series description of a perfect ellipse will be considered in greater detail in section 4.

Consider now a ring in which inner and outer profiles are no longer perfect ellipses. The departure from ellipticity can be defined using Fourier series as described in reference [2]. For the purposes of illustration and simplicity, consider here the case where the departure from the purely elliptical shape takes the form of a single spatial harmonic of amplitude $h_f^{\pm}$. In this case, the outer and inner profile functions, $f^+(\beta)$ and $f^-(\beta)$, can be expressed in terms of β as

$$f^+(\beta) = r^+ + h_f^+ \cos i\beta, \tag{5}$$

$$f^-(\beta) = r^- + h_f^- \cos(j\beta - \phi), \tag{6}$$

where ϕ is the spatial phase between the inner and outer profiles, $r^+ = \overline{OP_o}$ and $r^- = \overline{OP_i}$ respectively denote the distances from the coincident centres of the perfectly elliptical surfaces, on which the profile variations are superimposed, to points on the outer and inner surfaces at angle β, as shown in Figure 1(b).

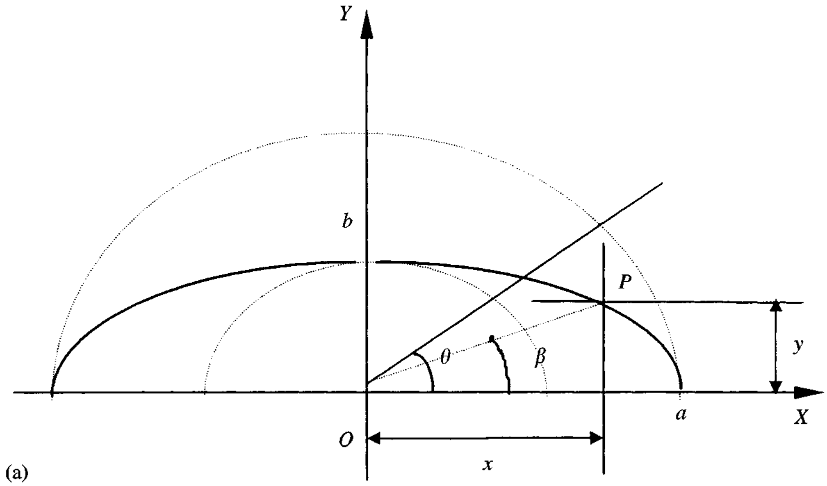

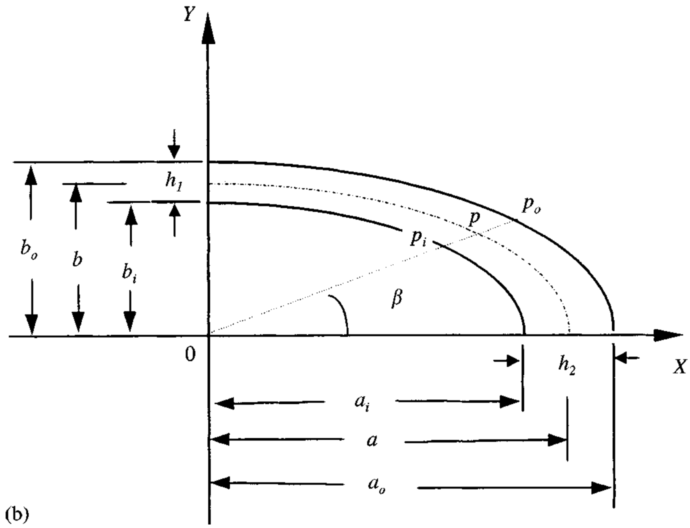

Figure 1. (a) The middle surface of an elliptical ring with constant cross-section. (b) An elliptical ring with variable cross-section.

These are given by

$$r^{+} = \frac{a_o b_o}{[a_o^2 \sin^2\beta + b_o^2 \cos^2\beta]^{1/2}}, \tag{7}$$

$$r^{-} = \frac{a_i b_i}{[a_i^2 \sin^2\beta + b_i^2 \cos^2\beta]^{1/2}}, \tag{8}$$

a_o, b_o, a_i and b_i are, respectively, the nominal semi-major and semi-minor axes of the outer and inner profiles.

Once the outer and inner surface functions, $f^{+}(\beta)$ and $f^{-}(\beta)$, are defined, the middle surface function $f(\beta)$ can be expressed in terms of a variable parameter m as

$$f(\beta) = mr^{+} + (1-m)r^{-} + mh_f^{+} \cos i\beta + (1-m)h_f^{-} \cos(j\beta - \phi), \tag{9}$$

where $0 < m < 1$ and $\beta = 0$ to 2π.

The variation of m with β can be determined using the iterative numerical procedure, which is described in detail in references [1, 2]. This allows the true midsurface to be determined, as required for proper implementation of the reduced Novozhilov shell theory [11], on which the strain and kinetic energy expressions will be based.

3. EIGENVALUE PROBLEM

For free vibration at frequency ω the tangential and normal displacements, v and w, of the middle surface are assumed to have the following forms:

$$v = \sum_{n=0}^{N} (v_n^s \sin n\beta - v_n^c \cos n\beta)\,\mathrm{e}^{\mathrm{i}\omega t} \tag{10}$$

$$w = \sum_{n=0}^{N} (w_n^c \cos n\beta + w_n^s \sin n\beta)\,\mathrm{e}^{\mathrm{i}\omega t}, \tag{11}$$

where v_n^c, v_n^s, w_n^c and w_n^s are the generalized co-ordinates and the superscripts "s" and "c" denote the coefficients of sine and cosine terms, respectively.

The relevant strain energy and kinetic energy calculations and subsequent application of the Rayleigh–Ritz method are fully described in reference [2] from which the eigenvalue problem can be expressed in the following form:

$$\left[\begin{bmatrix} \mathbf{K}^{ss} & \mathbf{K}^{sc} \\ \mathbf{K}^{cs} & \mathbf{K}^{cc} \end{bmatrix} - \lambda^2 \begin{bmatrix} \mathbf{M}^{ss} & \mathbf{M}^{sc} \\ \mathbf{M}^{cs} & \mathbf{M}^{cc} \end{bmatrix}\right] \begin{bmatrix} \mathbf{q}_s \\ \mathbf{q}_c \end{bmatrix} = \begin{bmatrix} \mathbf{0} \\ \mathbf{0} \end{bmatrix}, \tag{12}$$

where

$$\mathbf{q}_s = [v_0^S, w_0^S, v_1^S \ldots v_N^S, w_N^S]^T, \qquad \mathbf{q}_C = [v_0^C, w_0^C, v_1^C \ldots v_N^C, w_N^C]^T \tag{13}$$

and $[\mathbf{K}^{ss}]$, $[\mathbf{M}^{ss}]$, etc., represent stiffness and mass matrices of size $2(N+1)$ where N is the number of terms in the displacement function series (equations (10) and (11)). The frequency factors, $\lambda(n)$, are the eigenvalues of equation (12), which are calculated using standard numerical routines. They are defined by

$$\lambda(n) = \sqrt{\frac{\rho}{E}}\,\ell_0\,\omega(n), \tag{14}$$

where $\omega(n)$ is the natural frequency of the nth radial mode, ρ and E are density and Young's modulus respectively. ℓ_0 is a representative length, defined here as

$$\ell_0 = \frac{\sqrt{12}}{h_1} b^2, \tag{15}$$

where h_1 is the radial thickness of the cross-section at $X = 0$ (see Figure 1(b)) and b is the semi-minor axis of the nominal mid-surface.

4. NUMERICAL RESULTS

In the following sections, results will be presented for a number of different cases including elliptical rings of constant cross-section, elliptical rings of nominally constant cross-section with small additional profile variations and elliptical rings having a defined, variable cross-section. Natural frequency data is only presented for the low-order modes, which are likely to be of most practical significance.

The number of terms taken in the displacement function series, equations (10) and (11), governs the accuracy of the natural frequency prediction. In the present paper, 30 terms are used. This gives convergence to five significant figures in the frequencies of the second, third and fourth flexural modes. In the finite element analysis, a two-dimensional stress element is adopted and 120×2 elements are used for all the cases.

In order to compare the natural frequency factors calculated in the present study with those published in references [5, 7], the following nominal dimensions will be used (see Figure 1(b)): $a = 51$ mm with a/b in the range from 1/1·1 to 1/1·7 and $b = 51$ mm with a/b in the range from 1·0 to 2·0, $h_1 = 1$ mm with h_2/h_1 in the range 1·0–1·4.

4.1. ELLIPTICAL RINGS OF CONSTANT CROSS-SECTION

The results of the current study were derived using both the numerical method developed in references [1, 2] and the finite element method.

For illustration, Table 1 compares the results of the present study with those given in references [5, 7] for the cases of $h_2/h_1 = 1{\cdot}0$ and $a/b = 1{\cdot}1$–$2{\cdot}0$ for the 2nd and 4th symmetric modes. The results of the present study shown in Table 1 were obtained using exact functions to define the outer and inner profiles of the ring and the middle surface was calculated from the outer and inner profiles as described in reference [2].

It can be seen that the results obtained using the present numerical approach are in excellent agreement with the finite element results. The maximum difference is less than 0·5% for the $n = 2$ modes and less than 0·7% for the $n = 4$ modes. For $a/b \leqslant 1{\cdot}2$, good agreement (typically $< 2\%$ for $n = 2$ and 4) is obtained between the factors of the present study and those of references [5, 7]. As a/b increases from 1·4 to 2·0, the frequency factors obtained in reference [7] are still in good agreement ($\sim 2{\cdot}2\%$) with those of the present study. However, for larger values of a/b, there is an increasing divergence between the results of reference [5] and those of the present study and differences of the order of 85% (three-term polynomial series) and 120% (three-term sinusoidal series) are observed for the $n = 4$ modes, illustrating the limitations of a three-term displacement series as used in reference [5].

The variation in the natural frequency factors for flexural modes with $n = 2$ is illustrated graphically in Figure 2. The observed decrease in frequency factor with increasing aspect ratio a/b, is a result of the fact that the centreline length of the ring increases as a/b increases with b held at a constant value (see equation (15)).

The results in Table 1 also show that one of the effects of increasing the aspect ratio a/b is to produce frequency splitting between pairs of modes that would have

TABLE 1

Comparison of predicted frequency factors (λ) for the $n = 2$ and $n = 4$ modes for $h_2/h_1 = 1{\cdot}0$ and varying aspect ratio a/b

		Second mode					Fourth mode				
a/b	Symmetric or anti-symmetric mode	Present study (numerical)	Present study (FE)	Reference [7]	Reference [5] 3-S	Reference [5] 3-P	Present study (numerical)	Present study (FE)	Reference [7]	Reference [5] 3-S	Reference [5] 3-P
1·0	S	2·683	2·685	2·683	2·683	2·683	14·55	14·56	14·55	14·55	14·83
		(0·0)	(0·0)	(0·0)			(0·0)	(0·0)	(0·0)		
	A	2·683	2·685	2·683	—	—	14·55	14·56	14·55	—	—
1·1	S	2·426	2·428	2·427	2·427	2·432	13·16	13·18	13·17	13·18	13·32
		(0·33%)	(0·29%)	(0·4%)			($\approx$0·0)	($\approx$0·0)	(0·0%)		
	A	2·434	2·435	2·437	—	—	13·16	13·18	13·27	—	—
1·2	S	2·193	2·194	2·193	2·195	2·201	11·90	11·92	11·93	12·10	12·13
		(1·14%)	(1·19%)	(1·5%)			($\approx$0·0)	($\approx$0·0)	(0·0%)		
	A	2·218	2·220	2·226	—	—	11·90	11·92	11·93	—	—
1·4	S	1·795	1·797	1·801	1·820	1·813	9·771	9·790	9·834	11·04	10·57
		(4·1%)	(3·9%)	(4·7%)			(0·02%)	(0·02%)	(0·13%)		
	A	1·868	1·867	1·885	—	—	9·773	9·792	9·847	—	—
1·7	S	1·348	1·351	1·362	1·491	1·420	7·373	7·401	7·480	11·32	10·04
		(9·7%)	(9·6%)	(10·3%)			(0·11%)	(0·11%)	(0·51%)		
	A	1·479	1·482	1·518	—	—	7·381	7·409	7·519	—	—
2·0	S	1·034	1·039	1·056	1·362	1·219	5·687	5·728	5·813	12·63	10·65
		(16·5%)	(16·4%)	(19·2%)			(0·26%)	(0·26%)	(1·25%)		
	A	1·205	1·209	1·259	—	—	5·702	5·743	5·885	—	—

Note: Values in the parentheses represent the percentage frequency split, where available. 3-S and 3-P denote three-term sine series and three-term polynomial series respectively.

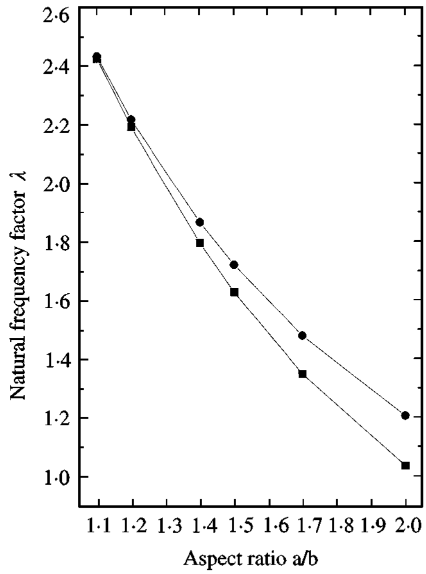

Figure 2. Natural frequency factors of perfectly elliptical ring in the 2nd radial mode. ——●—— higher mode; ——■—— lower mode.

identical natural frequencies in a perfectly circular ring. For example, the frequency factors of the symmetric and antisymmetric $n = 2$ modes are the same (2·683) when $a/b = 1$ but have a 16·5% split when $a/b = 2$. The $n = 4$ modes also show a frequency split, although less marked, as a/b increases. To help explain the observed pattern of behaviour we recall, as noted earlier, that the polar co-ordinate description of the ellipse, equation (4), can be expressed in terms of its spatial harmonic content, in a Fourier series of the form

$$r(\beta) = h_{09} + \sum_{p=1}^{\infty} [h_{pC} \cos p\beta + h_{pS} \sin p\beta]$$

References [1, 3] discuss the effect of spatial harmonics on frequency splitting in rings which depart from circularity and identify rules which govern splitting. The frequency splitting pattern in ellipses observed in Table 1 can be explained on the basis of these rules.

If one chooses the reference direction for β along the semi-major axis then, due to symmetry, all the Fourier coefficients except the even-harmonic cosine coefficients ($p = 2, 4, 6, \ldots$) will be zero. Table 2 shows the Fourier coefficients for ellipses with a/b in the range 1·1 to 1·4, normalized for $h_0 = 1$, and given to three decimal places. The corresponding percentage frequency splits for the first three sets of flexural modes are also given. It is clear from Table 2 that the Fourier coefficients decrease rapidly with increasing order. For example, for $a/b = 1{\cdot}4$, h_2 is 16·5% of h_0 and h_4 is 2% of h_0. For smaller values of a/b, the coefficients are much smaller. The observed pattern of frequency splitting is consistent with the splitting rules outlined in reference [3] which show that for even-harmonic profile variations (p even), there will be frequency splitting in modes of a given harmonic number n when $n = kp/2$

TABLE 2

Fourier coefficients h_i for ellipses of varying aspect ratio and corresponding frequency splits, $\Delta f(n)$, in modes with n nodal diameters

a/b	1·1	1·2	1·4
h_0	1·00	1·00	1·00
h_2	0·005	0·092	0·165
h_4	0·002	0·006	0·021
h_6	—	—	0·003
h_8	—	—	—
Mode no.		$\Delta f(n)$ (%)	
$n = 2$	0·32	1·16	3·78
$n = 3$	0·004	0·034	0·208
$n = 4$	—	—	0·019

($k = 1, 2, 3, \ldots$) with the largest effect when $k = 1$. The largest split occurs in the second ($n = 2$) flexural modes and it is likely [4] that this is a most strongly associated with the relatively small h_4 coefficient and also, less strongly, with the rather larger h_2 coefficient. The frequency split in the $n = 3$ modes is related principally to the small h_6 profile coefficient. For the range of values of a/b illustrated, the spatial harmonic content of the elliptical profile is such that frequency splitting in the higher modes is very small ($< \sim 0{\cdot}02\%$). It is interesting to note that, if the ellipses are described by Fourier series then, for $a/b = 1{\cdot}1$, only the first four non-zero harmonics ($p = 2, 4, 6, 8$) are needed to give five significant figure agreement with the frequency factors calculated using the exact profile. For $a/b = 1{\cdot}4$, seven harmonics give the same level of agreement.

4.2. ELLIPTICAL RING WITH SMALL PROFILE VARIATIONS

The frequency splitting in perfect, uniform thickness elliptical rings caused by the spatial-harmonic content of the elliptical profile was considered in the previous section. Now consider the effects of small imperfection in the basic profile in the form of additional single-harmonic contributions, as described by equations (5) and (6). In addition to purely academic interest, these results are relevant when considering the accuracy of any experimentally measured frequencies because they demonstrate the possible magnitude of the changes in actual natural frequencies (compared to ideal "perfect ellipse" predictions) due to imperfection in the ring profile.

For illustration, results are presented for three different profile harmonic numbers ($i = j = 2, 3, 4$) and two values of spatial phase ($\phi = 0$, ϕ, π), representing the limiting cases of a ring of constant in-plane thickness but with centreline distorted from purely elliptical and a ring which retains an elliptical centreline but

TABLE 3

Comparison of predicted frequency factors (λ) for $n = 2$ modes for elliptical rings of varying aspect ratio with superimposed single harmonic profile variation

Profile type		Aspect ratio a/b					
		1·1	1·2	1·4	1·5	1·7	2·0
Perfect ellipse	H	2·434	2·218	1·868	1·721	1·479	1·205
		(0·33%)	(1·1%)	(4·1%)	(5·7%)	(9·7%)	(16·5%)
	L	2·426	2·193	1·795	1·628	1·348	1·034
	H	2·432	2·215	1·862	1·717	1·475	1·202
$i = j = 2$		(0·29%)	(1·1%)	(3·8%)	(5·6%)	(9·6%)	(16·4%)
$\phi = 0$	L	2·425	2·191	1·793	1·626	1·346	1·033
	H	2·472	2·264	1·914	1·783	1·558	1·292
$i = j = 2$		(2·6%)	(1·8%)	(1·2%)	(3·2%)	(7·8%)	(15·7%)
$\phi = \pi$	L	2·409	2·224	1·891	1·727	1·445	1·117
	H	2·434	2·218	1·866	1·721	1·479	1·206
$i = j = 3$		(0·33%)	(1·1%)	(4·0%)	(5·7%)	(9·7%)	(16·5%)
$\phi = 0$	L	2·426	2·193	1·795	1·628	1·348	1·035
	H	2·400	2·184	1·832	1·688	1·447	1·176
$i = j = 3$		(0%)	(0·6%)	(2·9%)	(4·5%)	(8·2%)	(14·7%)
$\phi = \pi$	L	2·400	2·171	1·780	1·615	1·337	1·025
	H	2·440	2·223	1·868	1·722	1·480	1·206
$i = j = 4$		(0·87%)	(1·6%)	(4·3%)	(6·0%)	(10·0%)	(16·6%)
$\phi = 0$	L	2·419	2·187	1·791	1·624	1·345	1·034
	H	2·645	2·394	1·966	1·786	1·482	1·140
$i = j = 4$		(27·0%)	(25·7%)	(21·2%)	(18·5%)	(12·4%)	(3·4%)
$\phi = \pi$	L	2·083	1·905	1·622	1·507	1·318	1·102

Note: (i) "H" and "L" denote high and low frequency factors respectively.
(ii) Values in parentheses are percentage split between high and low frequency factors.

has harmonic variations in thickness around the circumference. Intermediate values of ϕ between 0 and π represent rings with distortions in both the centreline and in the in-plane thickness. This leads to frequency predictions that lie between the two limiting cases [1]. For illustration, the amplitude of the profile variation is taken to be $h_1 = 0{\cdot}1h$ where h is the mean thickness. The effects of varying h_1 for nominally circular rings are reported in references [1, 4].

The natural frequency factors for modes with $n = 2$ and 3 are presented in Tables 3 and 4, respectively, for a ring with the above profile variations for aspect ratios a/b in the range 1·1–2·0 and $h_2/h_1 = 1{\cdot}0$. The tabulated data shows that the variations in natural frequency factors, and the degree of frequency splitting, depend both on the profile variation and on the aspect ratio of the ring. The patterns of behaviour are best illustrated graphically and the main points are discussed below with reference to Figures 2–5. For reference, Figure 2 shows the

TABLE 4

Comparison of predicted frequency factors (λ) for $n = 3$ modes for elliptical rings of varying aspect ratio with superimposed single harmonic profile variation

Profile type		Aspect ratio a/b					
		1·1	1·2	1·4	1·5	1·7	2·0
Perfect ellipse	H	6·860	6·196	5·065	4·592	3·800	2·916
		(0·00%)	(0·03%)	(0·2%)	(0·35%)	(0·725)	(1·3%)
	L	6·860	6·194	5·055	4·576	3·773	2·878
	H	6·856	6·189	5·056	4·583	3·791	2·910
$i = j = 2$		(0·01%)	(0·05%)	(0·23%)	(0·39%)	(0·77%)	(1·4%)
$\phi = 0$	L	6·855	6·186	5·044	4·565	3·762	2·869
	H	6·880	6·262	5·173	4·714	3·943	3·068
$i = j = 2$		(0·17%)	(0·27%)	(0·06%)	(0·23%)	(1·1%)	(2·6%)
$\phi = \pi$	L	6·868	6·245	5·170	4·703	3·902	2·990
	H	6·860	6·196	5·065	4·591	3·800	2·918
$i = j = 3$		(0·00%)	(0·03%)	(0·20%)	(0·33%)	(0·72%)	(1·4%)
$\phi = 0$	L	6·860	6·194	5·055	4·576	3·773	2·879
	H	6·888	6·219	5·078	4·598	3·794	2·899
$i = j = 3$		(3·0%)	(2·9%)	(2·7%)	(2·6%)	(2·4%)	(2·2%)
$\phi = \pi$	L	6·690	6·045	4·943	4·480	3·705	2·838
	H	6·860	6·196	5·064	4·590	3·797	2·922
$i = j = 4$		(0·03%)	(0·07%)	(0·27%)	(0·41%)	(0·77%)	(1·4%)
$\phi = 0$	L	6·859	6·192	5·051	4·571	3·768	2·881
	H	6·794	6·149	5·051	4·589	3·813	2·9389
$i = j = 4$		(0·20%)	(0·38%)	(0·71%)	(0·84%)	(1·1%)	(1·1%)
$\phi = \pi$	L	6·780	6·125	5·015	4·550	3·773	2·906

Note: (i) "H" and "L" denote high and low frequency factors, respectively.
(ii) Values in parentheses are percentage split between high and low frequency factors.

natural frequencies for $n = 2$ modes of an elliptical ring without profile variations for $a/b = 1·1–2·0$.

As noted previously, the frequency factors of all modes fall significantly as a/b increases from 1 to 2 because with b constant, the circumferential length of the ring is increasing. Regarding the pairs of modes for which $n = 2$ (Table 3) it can be seen that, in general terms, the changes in frequency factor due to profile variation are in most cases quite small.

For the cases where $i = j = 2$, $i = j = 3$, and $\phi = 0$, the plots of frequency factor against a/b would be visually identical to Figure 2. In fact, for $i = j = 3$, $\phi = 0$, the frequency factors are numerically identical to those of the perfect ellipse to within the accuracy of the presented data. This is consistent with the frequency splitting rules given in reference [3].

For $i = j = 4$ and $\phi = 0$, there is a noticeable difference compared with the perfect ellipse for values of a/b close to unity (e.g. 0·87% split compared to 0·33%

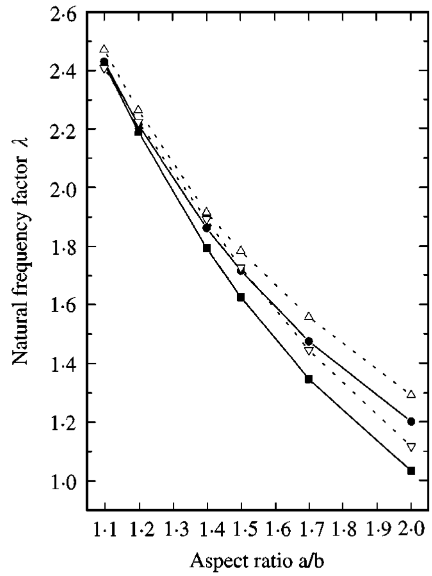

Figure 3. Natural frequency factors of perfectly elliptical ring and elliptical ring with $i = j = 2$ profile variation for the 2nd radial mode. $\phi = \pi$. Perfect ellipse: ——●—— higher mode; ——■—— lower mode. Ellipse with profile variation: - - △- - higher mode; - - ▽ - - lower mode.

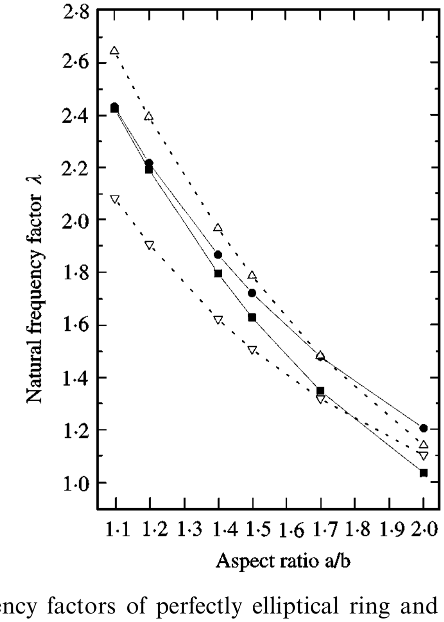

Figure 4. Natural frequency factors of perfectly elliptical ring and elliptical ring with $i = j = 4$ profile variation for the 2nd radial mode. $\phi = \pi$. Perfect ellipse: ——●—— higher mode; ——■—— lower mode. Ellipse with profile variation: - - △- - higher mode; - - ▽ - - lower mode.

split for $a/b = 1{\cdot}1$). This behaviour is generally consistent with the observations regarding nominally circular rings reported in reference [3]. When the spatial phase is zero (constant thickness) the $i = j = 2, 3$ profile variations do not interact strongly with the $n = 2$ modes but $i = j = 4$ profile variations interact more

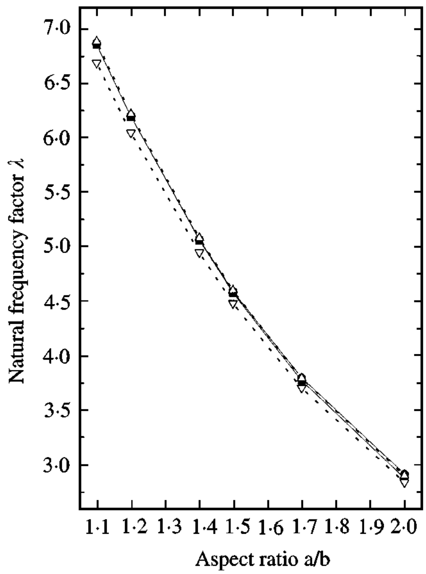

Figure 5. Natural frequency factors of a perfectly elliptical ring and elliptical ring with $i = j = 3$ profile variation for the 3rd radial mode. $\phi = \pi$. Perfect ellipse: ——●—— higher mode; ——■—— lower mode. Ellipse with profile variation: - - △- - higher mode; - - ▽ - - lower mode.

strongly. For values of a/b close to unity, the $i = j = 4$ profile variations cause additional frequency splitting compared with the perfect ellipse, but at larger values of a/b the behaviour is dominated by the aspect ratio effects.

The pattern of behaviour for $n = 2$ modes is somewhat different when the spatial phase $\phi = \pi$, and greater deviations in the frequency factors are noted compared with the perfect ellipse. Figure 3 compares the case where $i = j = 2$, $\phi = \pi$ with the perfect ellipse. At low aspect ratios ($a/b \sim 1$), the effect of profile variation is to significantly increase the frequency split from 0·33 to 2·6%. As the aspect ratio is increased towards 2·0, the frequency factors are higher than those for a perfect ring (e.g. 1·292 compared to 1·205) but the percentage frequency split is of the same order although slightly smaller. Clearly, the overall pattern of behaviour is influenced by a combination of thickness variation and aspect ratio effects while the (undeformed) ring centreline remains perfectly elliptical. For $i = j = 3$, $\phi = \pi$, the trend is almost identical to that of a perfect ellipse, but with a slight reduction (1·4–2·4%) in the frequency factors as a/b increases. The most significant changes to the natural frequency factors of $n = 2$ modes are found to occur for $i = j = 4$, $\phi = \pi$, as in Figure 4. Here, it can be seen that the presence of the profile variation reverses the trend of frequency splitting. Very large frequency splits ($\sim$27%) occur at low aspect ratios ($\sim$1·1). As the aspect ratio increases towards 2·0, the frequency split reduces to a lower value ($\sim$3·4%) than that of the perfect ellipse ($\sim$16·5%). Thus, at low values of a/b, the profile variation dominates the frequency split (consistent with observed behaviour of circular rings) but at higher values of a/b the balance between profile variation and aspect ratio effects is such that frequency splitting is much reduced. Regarding the $n = 3$ modes (Table 4), relatively small variations in the frequency factors are again observed in most cases. The most significant case considered is $i = j = 3$, $\phi = \pi$, see Figure 5, which introduces relatively large ($\sim$3%) frequency splits at low values of a/b and causes the frequency split to be increased significantly for all values of a/b considered.

The above discussion may be summarized as follows. The changes introduced in the lowest modes due to low-order harmonic variations in the profile are generally quite small. In all cases, the overall result is due to a balance of profile variation and aspect ratio effects, but the contribution from profile effects is generally in accordance with the patterns outlined in reference [3]. For rings which are close to circular ($a/b \sim 1$), the effect of thickness variation tends to dominate the frequency split but at higher aspect ratios the effect of lack of circularity becomes the dominant feature.

4.3. ELLIPTICAL RING WITH VARIABLE CROSS-SECTION

Reference [5] presents results for the symmetric flexural modes of inextensible, non-uniform elliptical rings with two planes of symmetry, in which the in-plane thickness varies linearly along the section centreline in each quadrant (see Figure 1(b)). The displacement was described using two different functions (three-term sinusoidal and optimized three-term polynomial). In the present study, an exact function was used to describe the outer and inner surfaces. Both the developed numerical method [1, 2] and the finite element method were used for h_2/h_1 in the range 1·0–1·4 and a/b in the range 1/1·7–2·0. The results presented here amplify and extend the results of reference [5] by including antisymmetric modes.

Table 5 gives a comparison between the natural frequency factors for $n = 2$ modes obtained by the present study, and those given in reference [5]. The most important features of the results can be summarized as follows.

The natural frequency factors obtained using the current numerical analysis and the finite element method are in excellent agreement, the maximum difference being less than 1% in the studied cases. The three-term sinusoidal approximation of reference [5] gives good agreement with the finite element predictions with a difference of less than 5·5% for $1/1{\cdot}5 < a/b < 1{\cdot}2$. However, for more extreme values of a/b, the discrepancy increases significantly to $\sim$21% for $a/b = 1{\cdot}4$. A similar pattern of behaviour is displayed for the three-term polynomial series of reference [5], but the percentage differences are less by a factor of about two in most cases. Clearly, an increased number of terms in the displacement approximation series would give better accuracy.

The general trends in the frequency factors given in Table 5 may be summarized as follows. The frequency factors are affected both by aspect ratio (a/b) variations and thickness ratio (h_2/h_1) variations. Generally, all frequency factors increase as thickness ratio increases (with h_1 constant) and decrease as a/b increases (with b constant). However, for the range of parameters considered, aspect ratio variations make a larger contribution to the change of frequency factors. For example, compared with a circular ring of uniform thickness ($a/b = 1$, $h_2/h_1 = 1$), a change in aspect ratio to $a/b = 1{\cdot}4$ produces $\sim$33% change in the $n = 2$

TABLE 5

Comparison of predicted frequency factors (λ) for $n = 2$ modes for elliptical rings of varying aspect ratio with variable thickness ratio h_2/h_1

Method	h_2/h_1	a/b S/A	1/1·7	1/1·4	1·0	1·4	1·7	2·0
Current numerical	1·0	S	4·05	3·65	2·683	1·80	1·35	1·03
		A	4·54	3·87	2·683	1·87	1·48	1·21
	1·1	S	4·06	3·67	2·82	1·90	1·43	1·09
		A	4·53	3·86	2·81	1·94	1·53	1·25
	1·2	S	4·22	3·82	2·95	2·00	1·51	1·16
		A	4·78	4·06	2·94	2·02	1·59	1·28
	1·3	S	4·38	3·98	3·09	2·10	1·59	1·21
		A	5·02	4·25	3·05	2·08	1·63	1·32
	1·4	S	4·54	4·13	3·23	2·21	1·66	1·27
		A	5·25	4·43	3·17	2·15	1·68	1·35
Finite element	1·0	S	—	—	2·685	1·80	1·35	1·04
		A	—	—	2·685	1·87	1·48	1·21
	1·1	S	4·06	3·67	2·82	1·90	1·43	1·10
		A	4·54	3·87	2·82	1·94	1·53	1·25
	1·2	S	4·22	3·83	2·96	2·00	1·51	1·16
		A	4·79	4·06	2·94	2·02	1·59	1·29
	1·3	S	4·38	3·98	3·09	2·11	1·59	1·22
		A	5·03	4·25	3·06	2·08	1·64	1·32
	1·4	S	4·55	4·13	3·23	2·21	1·67	1·28
		A	5·26	4·43	3·17	2·15	1·68	1·36
Laura 3-S	1·1	S	4·18	3·67	2·81	2·02	—	—
	1·2	S		3·79	2·95	2·24	—	—
	1·3	S		3·91	3·08	2·46	—	—
	1·4	S		4·03	3·21	2·68	—	—
Laura 3-P	1·1	S	4·14	3·70	2·81	1·92	1·51	—
	1·2	S	4·28	3·85	2·95	2·02	1·62	—
	1·3	S	4·43	4·00	3·08	2·13	1·72	—
	1·4	S	4·57	4·15	3·21	2·24	1·83	—

frequency factors. By comparison, a change in thickness ratio to $h_2/h_1 = 1{\cdot}4$ produces $\sim$19% change in the frequency factors. The magnitude of frequency splitting also depends on the combined effects of thickness variations and eccentricity, but the aspect ratio is more influential in the range of parameters considered. For example, with $a/b = 1$ (circular ring) the frequency splitting in the $n = 2$ modes varies from 0 to $\sim$1·9% as h_2/h_1 varies from 1·0 to 1·4. However, for $h_2/h_1 = 1$ (constant thickness), the frequency splitting varies in the range 0 to $\sim$17·5% as a/b varies in the range 1/1·7–2·0. The fact that the thickness variation produces relatively little effect on the frequency split of the $n = 2$ modes may be interpreted intuitively on the basis that the assumed linear variation in thickness in each quadrant of the ring produces a predominantly 2θ thickness variation, which does not interact strongly with $n = 2$ modes [4].

The effects of additional, single-harmonic profile variations on the variable thickness ellipse described above are considered in reference [1].

5. CONCLUSIONS

The free vibrations of nominally elliptical rings having constant or variable cross-section have been investigated. The study has made use of a numerical method that takes proper account of the true mid-surface of the ring. For comparison, results have also been obtained using the finite element method. The results obtained by the numerical method and the finite element method show excellent agreement.

The effect of the aspect ratio of the ellipse on frequency splitting between modes has been investigated in terms of a Fourier series description of the profile of the ellipse. The behaviour is shown to match previously observed patterns. The influence of single harmonic perturbations on the ring profile has also been investigated and the resulting patterns of frequency splitting have been explained.

Comparison of the predictions of the current numerical method with previously published results for rings of variable thickness shows good agreement for rings with aspect ratios close to unity. However, when the aspect ratio is significantly different from unity, the additional terms used in the present work, together with the accurate determination of the true middle surface, give results of significantly improved accuracy. The relative effects of aspect ratio variations and thickness ratio variations on the behaviour of the frequency factors has been highlighted.

REFERENCES

1. R. Hwang 1997 *Ph.D. Thesis, University of Nottingham, U.K.* Free vibrations of thin rings with profile variations.
2. R. S. Hwang, C. H. J. Fox and S. McWilliam 1999 *Journal of Sound and Vibration* **220**, 497–516. The in-plane vibration of thin rings with in-plane profile variations. Part I: general background and theoretical formulation.
3. R. S. Hwang, C. H. J. Fox and S. McWilliam 1997 *The 6th International Conference on Recent Advances in Structural Dynamics, Southampton*, 1457–1470. The free, in-plane vibration of circular rings with small thickness variations.
4. C. H. J. Fox, R. S. Hwang and S. McWilliam 1999 *Journal of Sound and Vibration* **220**, 517–539. The in-plane vibration of thin rings with in-plane profile variation. Part II: application to nominally circular rings.
5. P. A. A. Laura, E. Bambill, C. P. Filipich and R. E. Rossi 1988 *Journal of Sound and Vibration* **126**, 249–254. A note on free vibrations of non-uniform elliptical ring in its plane.
6. G. A. Brigham 1973 *The Journal of the Acoustical Society of America* **54**, 451–460. In-plane free vibrations of tapered oval rings.
7. K. Sato 1975 *Journal of Acoustic Society of America* **57**, 113–115. Free flexural vibrations of an elliptical ring in its plane.

8. N. W. McLachlan 1964 *Theory and Application of Mathieu Functions*. New York: Dover.
9. K. Suzuki and A. W. Leissa 1985 *ASME Journal of Applied Mechanics* **52**, 149–154. Free vibrations of non-circular cylindrical shells having circumferentially varible thickness.
10. G. Yamada, T. Irie and S. Notoya 1985 *Journal of Sound and Vibration* **101**, 133–139. Natural frequencies of elliptical cylindrical shells.
11. V. V. Novozhilov 1959 *The Theory of Thin Shells*. Leiden: P. Noordhoff, first edition.